Low loss dual-wave laser optics coatings at 1060nm and 530nm

Jue Wang, Horst Schreiber

Corning Advanced Optic Development – Corning Specialty Materials

60 O'Connor Road, Fairport, New York, 14450-1376, USA

ABSTRACT

Red-to-green laser conversion requires dual-wave laser optics coatings at 1060nm and 530nm. Loss analysis of the dual-wave coatings were presented for 3 types of coating designs with a coating material combination of HfO_2/SiO_2. Homogeneity and smoothness of the HfO_2/SiO_2 multilayers via standard plasma ion assisted deposition were evaluated. A modified plasma ion assisted deposition process with in-situ plasma smoothing was developed to deposit dense and smooth HfO_2/SiO_2 multilayers. Improved film microstructure was revealed on single layer and multilayer coated samples by means of atomic force microscopy and scanning electron microscopy. The improved film microstructure led to low loss and laser durable coating performance.

Keywords: Laser optics, Dual-wave optical coatings, HfO_2/SiO_2 multilayer, Film characterization

1. Introduction

The advantages of laser sources and their wide range of applications require high performance laser optics in a wide spectral range from deep-ultraviolet (DUV) to long wavelength infrared (LWIR). Advanced optical coatings play a dominant role in the ability to use lasers to meet the demands of such applications. For example, dual-wave optical coatings at 1060nm and 530nm enhance red-to-green laser conversion efficiency. The green laser is obtained by using high nonlinearity $LiNbO_3$ crystal as second-harmonic generation (SHG) to convert an infrared laser diode at 1060nm to a synthetic green laser at 530nm.[1] The refractive index of the crystal is 2.144 and 2.223 at 1060nm and 530nm, corresponding to a reflectance loss of 13.2% and 14.4% at a normal angle of incidence on a single SHG surface, respectively. Dual-wave AR coatings at 1060nm and 530nm are necessary for both the input and output facets of the SHG. Other dual-wave coatings are also required to improve the green laser system performance. In addition, the

Window and Dome Technologies and Materials XII, edited by Randal W. Tustison, Proc. of SPIE
Vol. 8016, 80160Y · © 2011 SPIE · CCC code: 0277-786X/11/$18 · doi: 10.1117/12.883915

Downloaded From: http://proceedings.spiedigitallibrary.org/ on 05/28/2013 Terms of Use: http://spiedl.org/terms

laser durability of the dual-wave coatings needs to be considered. The input laser power can reach up to 500mW in CW mode focused on a 5μ waveguide, corresponding to a power density of $2MW/cm^2$. In this technical report, scatter loss of the dual-wave coatings at 530nm and 1060nm are analyzed. Surface and interface of the HfO_2/SiO_2 multilayer derived from plasma ion assisted deposition are revealed. Low loss dual-wave laser optics coatings are realized by introducing in-situ plasma smoothing.

2. Scatter loss of dual-wave coatings

A combination of HfO_2/SiO_2 was selected as the high and low refractive index materials for the dual-wave coating designs, due to their good thermal/mechanical stability and relatively high laser damage threshold.[2-5] Various amounts of surface and interfacial roughness were assumed, in order to estimate the scatter loss of the dual-wave coatings at 1060nm and 530nm. Fig. 1 plots scatter loss as a function of surface and interfacial roughness RMS (root-mean-square) for a dual-wave AR coating. Scatter loss increases with surface and interfacial roughness at both wavelengths. However, the ratio of the scatter loss at 530nm and 1060nm is 3.20 for a given RMS.

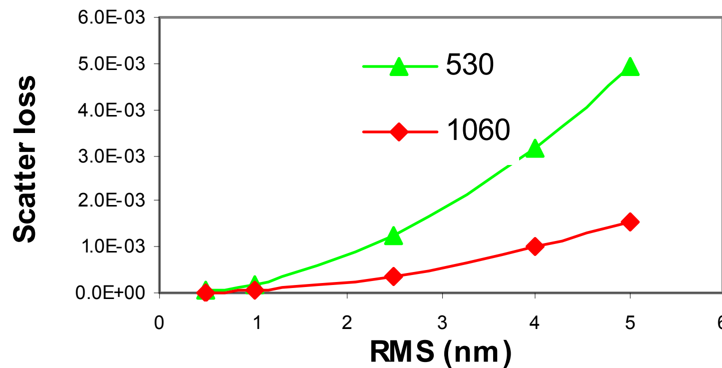

Fig. 1 Calculated scatter loss of a dual-wave AR coating @1060 & 530nm as a function of surface and interfacial roughness RMS.

Similar calculations were performed for a partial reflective coating at 1060nm combined with an antireflection coating at 530nm, i.e., PR@1060&AR@530, and for a high reflective coating at 1060nm and an antireflection coating at 530nm, i.e., HR@1060&AR@530. Fig. 2 depicts the

Downloaded From: http://proceedings.spiedigitallibrary.org/ on 05/28/2013 Terms of Use: http://spiedl.org/terms

scatter loss of the dual-wave coating PR@1060&AR@530 as a function of surface and interfacial roughness RMS. Fig. 3 describes the scatter loss of the HR@1060&AR@530 as a function of surface and interfacial roughness RMS. The ratio of the scatter loss at 530nm and 1060nm is 4.34 and 16.14 for the PR@1060&AR@530 and HR@1060&AR@530, respectively.

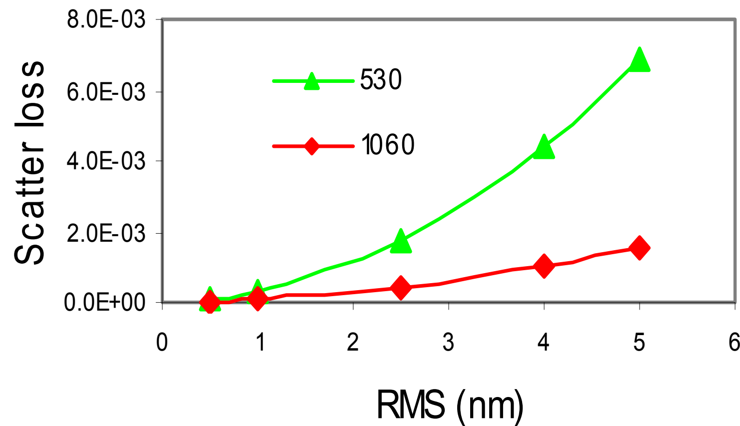

Fig. 2 Calculated scatter loss of dual-wave coating PR@1060nm and AR@530nm. as a function of surface and interfacial roughness RMS

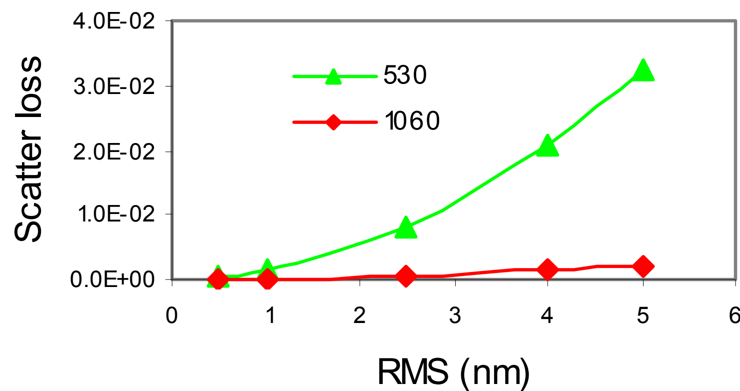

Fig. 3 Calculated scatter loss of dual-wave coating HR@1060nm and AR@530nm as a function of surface and interfacial roughness RMS.

Table 1 lists the scatter loss ratio SL@530/SL@1060 for the 3 different dual-wave coatings. The total number of layers of HfO_2/SiO_2 films is also included. As the total number of layers increases, the scatter loss ratio increases dramatically. Fig. 4 plots the spectral reflectance of the

Downloaded From: http://proceedings.spiedigitallibrary.org/ on 05/28/2013 Terms of Use: http://spiedl.org/terms

dual-wave coatings at an 8° angle of incidence. The dual-wave coatings were deposited on the output facets of the SHG to optimize red-to-green laser conversion efficiency and system performance.

Table 1 Scatter loss ration of dual-wave coatings

Dual-wave coating	AR@1060 & AR@530	PR@1060 & AR@530	HR@1060 & AR@530
SL@530/SL@1060	3.20	4.34	16.14
Total number of layers	4	6	25

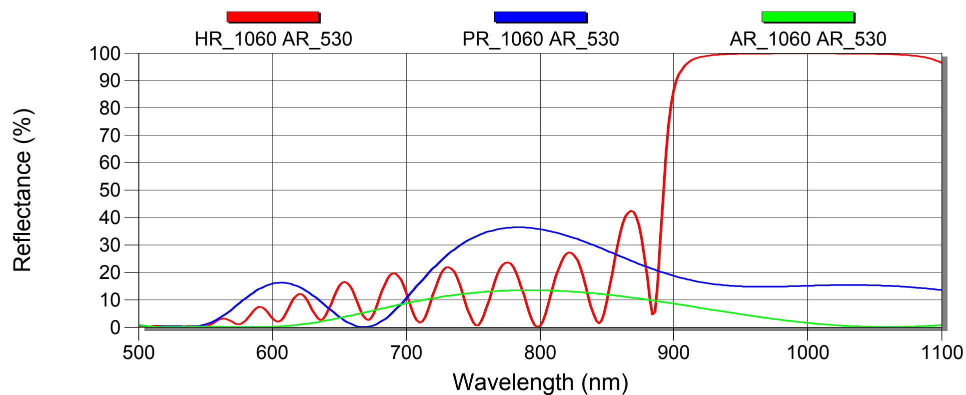

Fig. 4 Spectral reflectance of dual-wave coatings at 8° angle of incidence.

Low loss dual-wave coatings require multilayer HfO_2/SiO_2 with smooth surface and interfacial structure, especially for the dual-wave coating HR@1060&AR530. As seen in Fig.3 and Table 1, the scatter loss of the HR@1060&AR530 coating at 530nm is 16-fold greater than the scatter loss at 1060nm. A surface and interfacial roughness of 4nm in the dual-wave coating leads to a scatter loss of 0.13% and 2.1% at 1060nm and 530nm, respectively. As a result, achieving a high transmittance (>99.5%) at 530nm is a greater technical challenge than achieving a high reflectance (>99.5%) at 1060nm.

Downloaded From: http://proceedings.spiedigitallibrary.org/ on 05/28/2013 Terms of Use: http://spiedl.org/terms

3. Modified PIAD process

HfO_2/SiO_2 films were deposited via Leybold Syruspro 1110, equipped with an advanced plasma source (APS). The process was described in previous publications.[4-6] Two high purity raw materials, granular SiO_2 and hafnium metal, were irradiated by electron beams and thermally evaporated in high vacuum chambers. A rotating substrate holder located in the top of the chamber was negatively biased relative to the plasma source. Ions from the plasma sheet were accelerated to the substrates, bombarding the growing films while the electrons were reflected, resulting in plasma ion assisted deposition (PIAD). Oxygen gas was directly introduced into the vacuum chamber for chemically reactive deposition, whereas argon was used as a working gas for the plasma source.

A modified PIAD process includes standard plasma ion assisted deposition and in-situ plasma smoothing. Fig. 5 schematically illustrates the modified PIAD process, in which zone α and zone β correspond to the plasma smoothing and PIAD processes, respectively. Plasma momentum transfer of the modified PIAD process can be described by

$$P = (\alpha P_S + \beta P_D)(2\pi)^{-1} \qquad (1)$$

where P_S and P_D represent the amount of momentum transfer for the in-situ smoothing and the plasma ion assisted deposition, respectively.

The amount of plasma momentum transfer P_D used for assisting film deposition can be calculated by [2]

$$P_D = J_i (2 m_i e V_b)^{0.5} \gamma (R)^{-1} \qquad (2)$$

where R is the deposition rate in nm/sec, V_b is the plasma bias voltage, and J_i and m_i are the plasma ion flux in ion/(cm^2 sec) and mass in atomic units, respectively. e is the electron charge, and γ is a unit conversion factor.

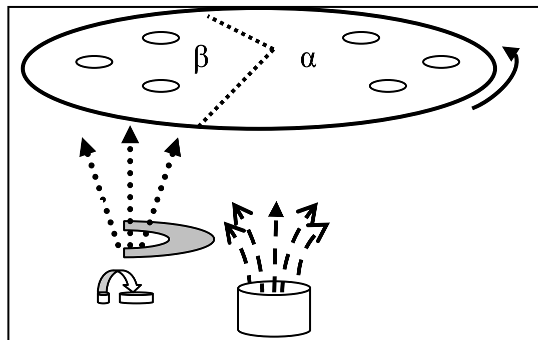

Hki 07'Uej go cvle'f tcy kpi 'qh'b qf khgf 'r ncuo c'kqp'cuukuvgf 'f gr qukkqp

Downloaded From: http://proceedings.spiedigitallibrary.org/ on 05/28/2013 Terms of Use: http://spiedl.org/terms

In addition to plasma assisted deposition, extra plasma interaction with the deposited film surface enables one to smooth film surfaces by increasing surface atom mobility and eliminating surface defects. The surface plasma smoothing effect can be described by the amount of plasma momentum transfer P_S ,

$$P_S = J_i (2m_i e V_b)^{0.5} \eta (n_s)^{-1} \qquad (3)$$

where n_s is the surface atom density of the deposited film in atom/cm^2, and η is a unit conversion factor. All other symbols have the same definition as Eq.(2).

3.1. Single layer HfO_2

Oxide film microstructure can be improved by means of advanced deposition techniques, such as ion assisted deposition (IAD), plasma ion-assisted deposition (PIAD), and ion-beam-assisted deposition (IBAD). For amorphous materials such as SiO_2, increasing plasma ion bombardment leads to film densification.[4-5] For materials with various phase structures, such as HfO_2, plasma ion bombardment may result in preferential film structure formation in addition to densification.[6]

The effectiveness of the in-situ smoothing was evaluated on single layer HfO_2 films with different PIAD processes. Fig. 6 shows AFM images of a 167nm HfO_2 film deposited on a commercial SiO2 substrate with the standard and modified PIAD processes. The RMS (root-mean-square) roughness obtained from AFM on sample L and sample R was 1.6nm and 0.4nm for the standard and modified PIAD, respectively. As can be seen on sample R, the substrate polish residual has been clearly transferred to the film surface from the substrate surface, indicating a dense and amorphous film growth mechanism. In the case of sample L, with the standard PIAD process, the substrate polish residual has disappeared from the film surface, because the morphology is dominated by the inhomogeneous film microstructure instead of the substrate. The inhomogeneous and homogeneous film structure of the HfO_2 films was also confirmed by ellipsometric measurement and data modeling, a nondestructive and surface sensitive optical method used to characterize thin films, surfaces, and material microstructures. [7-9]

Downloaded From: http://proceedings.spiedigitallibrary.org/ on 05/28/2013 Terms of Use: http://spiedl.org/terms

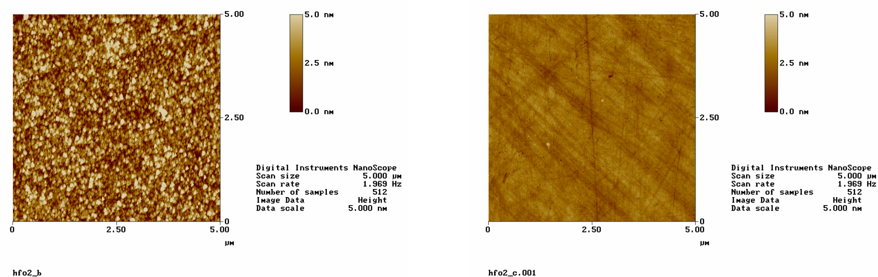

Fig. 6 AFM images of single layer of 167nm HfO_2 films deposited on SiO_2 substrates with standard (left image, sample L) and modified PIAD (right image, sample R).

3.2. HfO_2/SiO_2 multilayer

Following the HfO_2 single layer tests, HfO_2/SiO_2 multilayer deposition was conducted. Fig. 7 shows scanning electron microscopy (SEM) cross sectional images of the HfO_2/SiO_2 multilayer deposited from the standard PIAD process (top images) and the modified PIAD with in-situ plasma smoothing (bottom images). The layers with the light and gray colors represent the HfO_2 and SiO_2 layers, respectively. The HfO_2/SiO_2 films were deposited on SiO_2 substrates shown on the left of Fig. 7. The in-situ plasma smoothing process leads to film structure that is independent of total layer number and coating thickness, as revealed in the bottom images of Fig. 7. The typical surface roughness of the HfO_2/SiO_2 multilayer derived from the modified PIAD is less than 0.5nm. The surface roughness is independent of overall layer number and total film thickness. The modified PIAD enables low loss dual-wave coatings for green laser applications.

Downloaded From: http://proceedings.spiedigitallibrary.org/ on 05/28/2013 Terms of Use: http://spiedl.org/terms

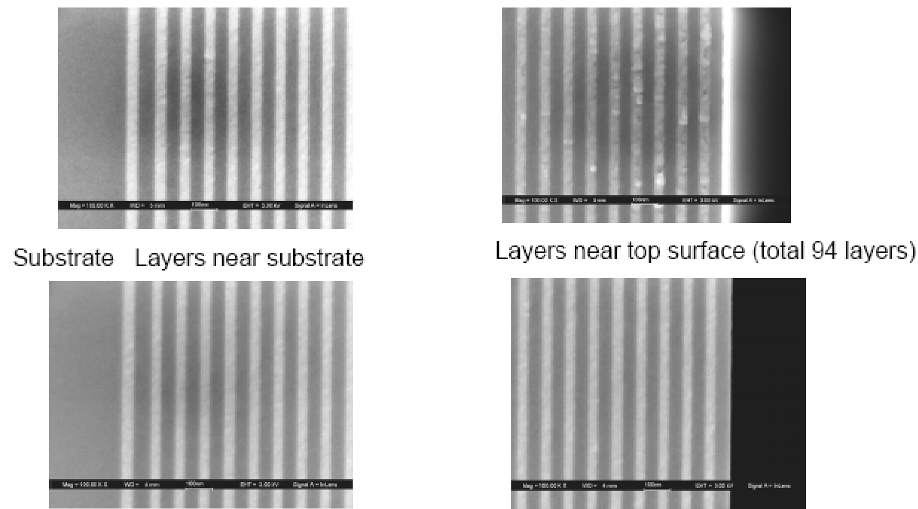

Fig. 7 SEM cross sectional images of HfO_2/SiO_2 multilayer deposited from standard PIAD process (top images) and modified PIAD (bottom images).

4. Conclusions

Loss analysis of dual-wave coatings was performed on 3 types of dual-wave coating designs with a coating material combination of HfO_2/SiO_2. The scatter loss of the dual-wave coatings was presented as a function of surface and interfacial roughness. A modified plasma ion assisted deposition process with in-situ plasma smoothing was developed to deposit dense and smooth HfO_2/SiO_2 multilayers. Improved film microstructure was revealed on single layer and multilayer coated samples by means of atomic force microscopy and scanning electron microscopy. The improved film microstructure led to low loss and laser durable coatings.

Acknowledgements

The authors would like to thank Ron Cheek for film deposition and Ronald W. Davis for SEM measurements. Angela Qu Wang's assistance in the manuscript preparation is greatly appreciated.

References

1. Vikram Bhatia, Anthony Bauco, Hassan Oubei, and David Loeber, "Green light allows big pictures from small projectors," SPIE Newsroom, 10.1117/2.120102.002636 (2011).

Downloaded From: http://proceedings.spiedigitallibrary.org/ on 05/28/2013 Terms of Use: http://spiedl.org/terms

2. Christopher J. Stolz, Michael D. Thomas, and Andrew J. Griffin, "BDS thin film damage competition," SPIE 7132, 71320C(2008).

3. R. Thielsch, A. Gatto, J. Heber, N. Kaiser, "A comparative study of the UV optical and structural properties of SiO_2, Al_2O_3, and HfO_2 single layers deposited by reactive evaporation, ion-assisted deposition and plasma ion-assisted deposition," Thin Solid Films 410, 86(2002).

4. Jue Wang, Robert L. Maier, Horst Schreiber, "Wavefront control of SiO_2-based ultraviolet narrow-bandpass filters prepared by plasma ion-assisted deposition," Applied Optics 46, 175(2007).

5. Jue Wang, Robert L. Maier, Horst Schreiber, "Elastic and plastic relaxation of densified SiO_2 films," Applied Optics 47(13), C189(2008).

6. Jue Wang, Robert L. Maier, Horst Schreiber, "Crystal phase transition of HfO_2 films evaporated by plasma ion-assisted deposition," Applied Optics 47(13), C131(2008).

7. Jue Wang, Robert L. Maier, "Surface assessment of CaF_2 DUV and VUV optical components by quasi-Brewster angle technique," Applied Optics 45, 5621(2006).

8. Jue Wang, Robert Maier, Paul G. Dewa, Horst Schreiber, Robert A. Bellman, David Dawson Elli, "Nano-porous structure of a GdF_3 thin film evaluated by variable angle spectroscopic ellipsometry," Applied Optics 46(16), 3221(2007).

9. Jue Wang, Steven VanKerkhove, Horst Schreiber, "Evaluation of coated and uncoated CaF2 Optics by variable angle spectroscopic ellipsometry," Thin Solid Films 519, 2881(2011).

Downloaded From: http://proceedings.spiedigitallibrary.org/ on 05/28/2013 Terms of Use: http://spiedl.org/terms